Available online at www.sciencedirect.com
SCIENCE DIRECT®
Biomaterials 27 (2006) 505–518
Biomaterials
www.elsevier.com/locate/biomaterials

Coil-reinforced hydrogel tubes promote nerve regeneration equivalent to that of nerve autografts

Yusuke Katayama[a], Rivelino Montenegro[a], Thomas Freier[a,c,d], Rajiv Midha[b,1], Jason S. Belkas[b], Molly S. Shoichet[a,c,d,*]

[a]*matREGEN Corporation, 200 College Street, Suite 28, Toronto, Ont., Canada M5S 3E5*
[b]*Sunnybrook and Women's College Health Sciences Centre, 2075 Bayview Ave., Toronto, Ont., Canada M4N 3M5*
[c]*Department of Chemical Engineering and Applied Chemistry, University of Toronto, 4 Taddle Creek Road, Room 407, Toronto, Ont., Canada M5S 3G9*
[d]*Department of Chemistry and Institute of Biomaterials and Biomedical Engineering, University of Toronto, 4 Taddle Creek Road, Room 407, Toronto, Ont., Canada M5S 3G9*

Received 6 July 2005; accepted 11 July 2005
Available online 25 August 2005

Abstract

Despite spontaneous sprouting of peripheral axons after transection injury, peripheral regeneration is incomplete and limited to short gaps, even with the use of autograft tissue, which is considered to be the "gold" standard. In an attempt to obviate some of the problems associated with autografts, including limited donor tissue and donor site morbidity, we aimed to synthesize a synthetic nerve guidance channel that would perform as well as the nerve autograft. Given that the patency of the nerve guidance channel is critical for repair, we investigated a series of nerve guidance channel designs where patency and the resulting regenerative capacity were compared in a transected rat sciatic nerve injury model. Three tube designs were compared to autograft tissue: plain, corrugated and coil-reinforced tubes of poly(2-hydroxyethyl methacrylate-*co*-methyl methacrylate). Of the three designs, the coil-reinforced tubes demonstrated superior performance in terms of patency. By electrophysiology and histomorphometry, the coil-reinforced tubes demonstrated outcomes that were comparable to autografts after both 8 and 16 weeks of implantation. The nerve action potential (NAP) velocity and muscle action potential (MAP) velocity for the coil-reinforced PHEMA-MMA tube was 54.6 ± 10.1 and 10.9 ± 1.3 m/s, respectively at 16 weeks, which was statistically equivalent to those of the autograft at 37.5 ± 7.9 and 11.3 ± 2.0 m/s. The axon density in the coil-reinforced tube was $2.16 \pm 0.61 \times 10^4$ axons/mm^2, which was statistically similar to that of the autograft of $2.41 \pm 0.62 \times 10^4$ axons/mm^2 at 16 weeks. These coil-reinforced tubes demonstrated equivalence to autografts for nerve regeneration, demonstrating the importance of channel design to regenerative capacity and more specifically the impact of patency to regeneration.

Keywords: Peripheral nerve regeneration; PHEMA; Patency; Tissue engineering

1. Introduction

Spinal cord injury results from either compression of the cord by, for example, vertebrate fracture, or cord transection due to a stabbing or gunshot wound. Severed spinal tissue lacks the capacity to regenerate due to the secretion of inhibitory and neurodegenerative molecules after injury, the presence of a glial scar, induction of apoptosis, lack of neuroregenerative

*Corresponding author. Department of Chemical Engineering and Applied Chemistry, University of Toronto, 4 Taddle Creek Road, Room 407, Toronto, Ont., Canada M5S 3G9. Tel.: +1 416 978 1460; fax: +1 416 978 4317.
E-mail address: molly@ecf.utoronto.ca (M.S. Shoichet).
[1]Current address: Division of Neurosurgery, Department of Clinical Neurosciences and Neuroscience Research Group, University of Calgary, Calgary, Alberta, Canada.

0142-9612/$ - see front matter © 2005 Elsevier Ltd. All rights reserved.
doi:10.1016/j.biomaterials.2005.07.016

molecules and the lack of a pathway along which regeneration could be stimulated [1]. The use of entubulation or guidance channels has been investigated by us using biostable PHEMA-MMA tubes [2] and others using biostable PAN/PVC [3–5] to promote regeneration of the transected spinal cord. Interestingly, most spinal cord entubulation repair strategies have studied non-degradable tubes, such as PHEMA-MMA and PAN/PVC, described above; however, some studies have investigated degradable tubes [6], yet with limited success, possibly due to the instability of the tube during regeneration or the swelling of the tube during degradation. Although the regenerative capacity of the central nervous system is not as profound as that of the peripheral nervous system, both systems require chemotactic cues and appropriate guidance for axonal growth. Thus the peripheral nervous system can be thought of as a model system for spinal cord repair. While repair in the PNS is spontaneous (and it is not in the CNS), repair of the peripheral nerve presents a simpler surgical site and allows many of the design criteria to be more rapidly tested than would be possible in the spinal cord. Thus in this study, where our focus is tube design and determining the optimal design for long-term patency, we investigated regeneration of the rat peripheral sciatic nerve.

After peripheral nerve injury, Wallerian degeneration is observed in the distal end of the injured axon, followed by spontaneous sprouting of fibres from the proximal stump to reinnervate the distal nerve [7–9]. However, depending on the size of the injury gap and the formation of neuroma and scar tissue, spontaneous reinnervation fails, requiring surgical intervention to bridge the gap. Short gaps, less than 1 cm in humans, can be repaired by suturing the peripheral nerve ends together whereas longer gaps require an autograft [10–12]. While the autograft is considered the gold standard for nerve repair, it is plagued by numerous deficiencies, including inconsistent results, scar and neuroma pain, scarce availability of donor tissue and donor site morbidity, not to mention the additional surgery required to harvest the donor tissue. To overcome the limitations associated with autografts, several researchers, including ourselves, have investigated synthetic nerve guidance channel alternatives to autografts [13–22]; however, none of these, including commercially available guidance channels can effectively bridge gaps longer than 3 cm in humans, limiting their use to short gaps. Moreover, the in vivo performance is often sub-optimal as compared to the nerve autograft.

In recent studies we found that poly(2-hydroxyethyl methacrylate-*co*-methyl methacrylate) (PHEMA-MMA) nerve guidance channels demonstrated equivalent regenerative capacity to nerve autografts for 8 and 16 weeks, but in the 16-week samples, a minority of the channels were sub-optimal, giving rise to a bimodal population in regenerative capacity [23]. PHEMA-MMA has been used in medicine for over 25 years because of its biocompatibility. We have been able to tune the transport and mechanical properties of the hollow fibre PHEMA-MMA membrane used as the nerve guidance channel through control of the formulation [24,25]. However, it was these tubes that resulted in the bimodal regenerative capacity observed after 16 weeks when used to repair a severed rat sciatic nerve injury gap. We hypothesized that the mechanical integrity of our previous PHEMA-MMA tubes was insufficient to withstand long-term (i.e. 16 weeks) in vivo forces [17]. To overcome this limitation, we investigated a series of designs for the nerve guidance channel and specifically examined the regenerative capacity in corrugated wall tubes and coil-reinforced composite tubes vs. plain tubes and autografts in the transected rat sciatic nerve injury model. Both corrugation and coils are common designs used to reinforce tubes in industrial applications [26–32] and based on this precedence we chose to investigate these designs for improved patency in nerve repair. Moreover, we were already using a high monomer concentration (of 33 wt%) and were limited by monomer solubility from using greater percent solids and thus could not simply increase wall thickness to achieve sufficient modulus for patency. All tubes were "enhanced" with fibroblast growth factor-1 (FGF-1), dispersed with heparin in a dilute collagen gel because we previously demonstrated enhanced regeneration with this growth factor/matrix mixture [33].

2. Material and methods

All chemicals were purchased from Sigma-Aldrich Co. (Milwaukee, WI) and used as received unless otherwise noted. Water was distilled and deionized using Millipore Milli-RO 10 Plus and Milli-Q UF Plus (Bedford, USA) at 18 MΩ resistance.

2.1. Tube synthesis

A liquid–liquid centrifugal casting process (SpinFX®) was used to synthesize all PHEMA-MMA tubes as previously described by Dalton and Shoichet [24]. Briefly, 27.1% (v/v) HEMA, that had been spiked with 0.1% (v/v) of ethylene glycol dimethacrylate (EDMA), and 5.1% (v/v) of MMA were mixed with 0.1% (w/v) of ammonium persulfate (APS) and 0.1% (w/v) of sodium metabisulfate (SMBS) in deionized water. The solution was injected into one of a series of capped cylindrical moulds, which was then spun at 5000 rpm in a horizontally mounted drill (BDC6015, Caframo) for 3 h.

Plain tubes were synthesized in cylindrical glass moulds having a 1.8 mm inner diameter (ID). Corrugated tubes were synthesized in custom-made corrugated PMMA moulds having a 0.7 mm pitch. Coil-reinforced tubes were synthesized in cylindrical glass moulds fitted with custom-made poly(caprolactone) (PCL) coils having a fibre diameter of 110 μm.

Prior to implantation, all PHEMA-MMA tubes were extracted in 10% ethanol overnight, re-equilibrated in phosphate buffered saline (PBS), and sterilized by gamma irradiation at 2.5 MRad. Gas chromatography analysis of the ethanol after extraction had no detectable monomer, initiator, accelerator, or crosslinker.

2.2. Characterization of tubes

Tubes were characterized for morphology by scanning electron microscope (SEM) and for compressive strength by mechanical testing. Tube morphologies were analysed by SEM (Model S-570, Hitachi) under dry conditions. For SEM imaging, samples were cut to 2 mm, quenched in liquid nitrogen and freeze-dried. Dried scaffolds were attached with double-sided tape to microscopy sample studs and gold-coated for 50 s. The samples were then placed on the SEM stage for imaging. Operating conditions included a working distance of 15 mm and an accelerating voltage of 20 kV.

2.3. Mechanical testing

Transverse compression testing of the tubes was performed on a Biosyntech micromechanical tester in aqueous solution at 37 °C. Empty tubes, of all three configurations, i.e. plain, corrugated and coil reinforced configuration, were analysed (i.e., without addition of collagen and FGF-1). The length of all samples was 8 mm. The tube wall thickness was measured before testing. The crosshead speed was maintained at 0.6 mm/min. The compressive strengths of tubes were compared from the load–displacement curves of three measurements. Results are expressed as means ± standard deviations. Variance analysis using an ANOVA Single Factor test was used for the statistical analysis, with 95% confidence.

2.4. Enhanced tubes

The FGF-1 cocktail was prepared under sterile conditions in a laminar hood. The instruments and plastic-ware were either autoclaved or gamma irradiated, and the solutions were sterile filtered. All plastic-ware was coated with bovine serum albumin (BSA) by immersion in PBS solution containing BSA (5 mg/ml) for at least 2 h and then rinsed with 0.1 mg/ml BSA. After coating with BSA, the vials, pipette tips, and syringes were then air dried overnight in a laminar hood. FGF-1 was co-dissolved with heparin (181 USP units/mg, Sigma) in a 1:2500 ratio (v/v) to stabilize FGF-1. Dilute collagen solutions were prepared at 4 °C by mixing 0.425 ml of Vitrogen (3 mg/ml) with 0.475 ml of PBS. The final pH of the solution was adjusted to pH 7.4 with 0.1 M NaOH and 0.1 M HCl. One hundred microlitres of FGF-1/heparin were added to 900 μl of the chilled collagen solution (pH 7.4) and vortexed. Collagen solutions (0.7 ml) containing the dispersed FGF-1 were quickly transferred to BSA coated vials. Seven PHEMA-MMA tubes were filled with this "cocktail" and held in the BSA-coated vials at 37 °C before implantation. The sciatic nerve stumps were placed in either end of the gel-filled tube at implantation and because the gel was weak (and did not completely fill the tube lumen), insertion was facile and unobstructed.

2.5. Implantation in the rat sciatic nerve

The "enhanced" PHEMA-MMA tubes were implanted as nerve guidance channels, bridging a 10 mm gap in the sciatic nerve of inbred adult male Lewis rats (250–275 g, Harlan Sprague Dawley, Indianapolis, IN), as previously described [23]. Canadian Council on Animal Care guidelines were strictly followed for all animal operations. Standard microsurgical operations were performed under an operating microscope (Leica M651, Leica Microsystems). Briefly, after administering anesthesia (xylazine and ketamine hydrochloride) and shaving and cleaning the incision area, gluteal and posterior thigh incisions were made to expose the sciatic nerves deep to the biceps femoris muscle, allowing a 7 mm segment of the nerve to be excised, which resulted in a 10 mm gap after the spontaneous retraction of the transected nerve.

For the tube groups, one animal received either 12 mm long plain, corrugated or coil-reinforced tubes in both sides of the sciatic nerve gap with each nerve end inserted 1 mm into the tube lumen and sutured in place with two 10-0 nylon sutures (Dermalon, Davis and Geck, American Cyanamid Company, Danbury, CT). Tubes were easily sutured in place and there was no evidence of tearing. A total of six tubes per type were implanted. For the autograft group, six sciatic nerve graft segments (10 mm long) were harvested from four isogenic Lewis donor rats. The harvested nerves were sutured into the gap of the recipient rats with 10-0 nylon epineurial sutures similar to the tube repair. Three animals received the grafts on both sides ($n = 6$). Muscle and skin incision wounds were closed by interrupted 3-0 Polysorb (Autosuture, Norwalk, CT) and continuous 3-0 silk (Autosuture, Norwalk, CT) sutures, respectively. Each rat received bilateral implantations.

2.6. Electrophysiology

At 8 and 16-week end-points, electrophysiological studies were performed prior to tissue harvesting as previously described [23]. Bipolar hooked platinum electroencephalographic stimulating electrodes were placed under the sciatic nerve 10 mm proximal to the injury site [34]. Recording electrode measured supramaximal evoked responses by placing one electrode under the sciatic nerve 10 mm distal to the graft end for nerve action potential (NAP) recording and reinnervated gastrocnemius muscle for muscle action potential (MAP) recording. The distances from the stimulating and recording sites proximal and distal from the graft were confirmed by using a calliper and a ruler. A ground electrode was placed in a superficial muscle layer near the skin. The conduction velocities of NAP and MAP were determined by a computer-assisted electromyographic machine (Cadwell 6200A, Cadwell Laboratories, Kennewick, WA). Conduction velocities were calculated from derived latencies and measured distances.

2.7. Histomorphometry

The mid portion of the tube graft and autograft and the distal portion of the sciatic nerve 5 mm from the suture line were harvested after 8 and 16 weeks. Tissues were fixed with a glutaraldehyde-based Universal Fixative, embedded with plastic, and sectioned on an ultramicrotome (Sorvall MT

6000, Ivan Sorvall, Norwalk, CT) to 1 μm thickness cross-sections. The sections were stained with toluidine blue and examined under the light microscope.

Seven pictures of high-powered fields (HPFs) (3092 μm^2, at a magnification of 1000×) were taken randomly and without overlapping, and myelinated axons with greater than 1 μm in diameter were selected for analysis. The tube walls, large blood vessels and epineurium were excluded from the pictures. As described previously [35], a colour-intensity-based method with the aid of Image Pro-Plus software (MediaCybernetics, Silver Spring, MD) was used to identify and measure the parameters of healthy myelinated axons in HPF pictures. The parameters measured include: (1) fibre diameter (entire myelinated axon diameter); (2) fibre area (entire myelinated fibre area); (3) G-ratio (a ratio of axon diameter to fibre diameter); (4) the ratio of axon area to myelin area; and (5) axon density (total number of axons per graft or the largest fascicle in the graft).

2.8. Lateral gastrocnemius dry muscle mass

The lateral gastrocnemius (LG) muscle mass was measured after 8 and 16 weeks of implantation as a gauge of degree of innervation [36]. After the excision, the LG muscle was dried by blotting on a paper towel and weighed on an electronic scale (Mettler AJ100, Mettler Instruments, Greifernsee-Zurich, Switzerland).

2.9. Statistical analysis

Data from electrophysiology, histomorphometry and muscle mass were analysed separately by a SigmaStat program (Systat Software, Point Richmond, CA). All electrophysiology parameters and muscle mass from 8 and 16 weeks were compared among the different tube configurations and autograft by one way ANOVA ($p<0.05$). When there was a statistically significant difference, pairwise multiple comparison procedures (Holm–Sidak method) were used to compare between two groups ($p<0.05$).

Based on the overall patency for 16-week explants and in vitro mechanical testing results, coil reinforced tubes were chosen for histomorphometric analysis and compared with the autograft. Histomorphometry parameters from 8 and 16 weeks were compared between two groups by independent sample *t*-tests using a 95% confidence interval ($p<0.05$).

3. Results

3.1. Morphological properties of tubes

To examine the role of patency more closely, we compared PHEMA-MMA tubes that were corrugated or reinforced with coils to plain tubes and autografts. Corrugated and coil-reinforced tubes, as shown in Fig. 1, were synthesized by the SpinFX® technology. Fig. 1A and B show the gross image of the corrugated and coil-reinforced tubes while Fig. 1C and D show the morphology within the tube wall of a longitudinal section of the corrugated and coil-reinforced tube, respectively. The wall morphology was found to be inhomogeneous in the corrugated tube wall (Fig. 1C), with smaller-sized pores at the zenith, larger size pores in the middle and no pores (or predominantly a gel-like structure) towards the tube lumen. The wall morphology in the coil-reinforced tube wall was mostly homogeneous in terms of pore size distribution, with the coil embedded in the wall structure easily visible. The plain tube consisted of an outer gel-like phase that made up the majority of the tube and an inner sponge-like phase [33].

Corrugated tubes had a wall thickness of 240 ± 10 and 430 ± 10 μm, corresponding to the peaks and valleys, respectively. Coil-reinforced tubes had a wall thickness of 220 ± 10 μm and a coil diameter of 110 ± 5 μm. The tubes were also compared in terms of mechanical properties, as shown in Fig. 2, where load vs. displacement data were collected at four displacements and the load measured. As shown, coil-reinforced tubes supported the greatest loads at all displacements, followed by corrugated tubes and then plain tubes, which had the lowest mechanical strength of the three tube types compared. These data demonstrate that both corrugated and coil-reinforced tubes were significantly stronger than plain tubes ($p<0.05$). Moreover, coil-reinforced tubes were significantly stronger than corrugated tubes ($p<0.05$).

3.2. Structural properties of tubes after implantation

The general morphology of the tubes were examined under the operating microscope after 8 and 16 weeks in vivo in terms of patency and were divided into three groups: round, oval and collapsed (i.e. 90% reduction of original tube ID), as summarized in Table 1. The coil-reinforced tubes performed the best, with all of the tubes remaining patent (or round) at both 8 and 16 weeks and all 16-week tubes having a regenerating cable. The corrugated and plain tubes demonstrated similar performance with each other in terms of patency and regenerating cable, with some differences noted. Both plain and corrugated tubes had a subset of tubes that were either oval or collapsed at 8 and 16 weeks, indicating a sub-optimal performance relative to the coiled tubes. Interestingly, corrugation did not improve patency over that of the plain tube.

3.3. Functional recovery

Electrophysiological measurements reflect the functional behaviour of the regenerated nerve, with the NAP velocity and the MAP velocity being the most relevant of the electrophysiological measurements studied for regenerative capacity [37]. As shown in Fig. 3, there were no statistically significant differences in mean NAP velocity after 8 weeks in vivo between all groups studied,

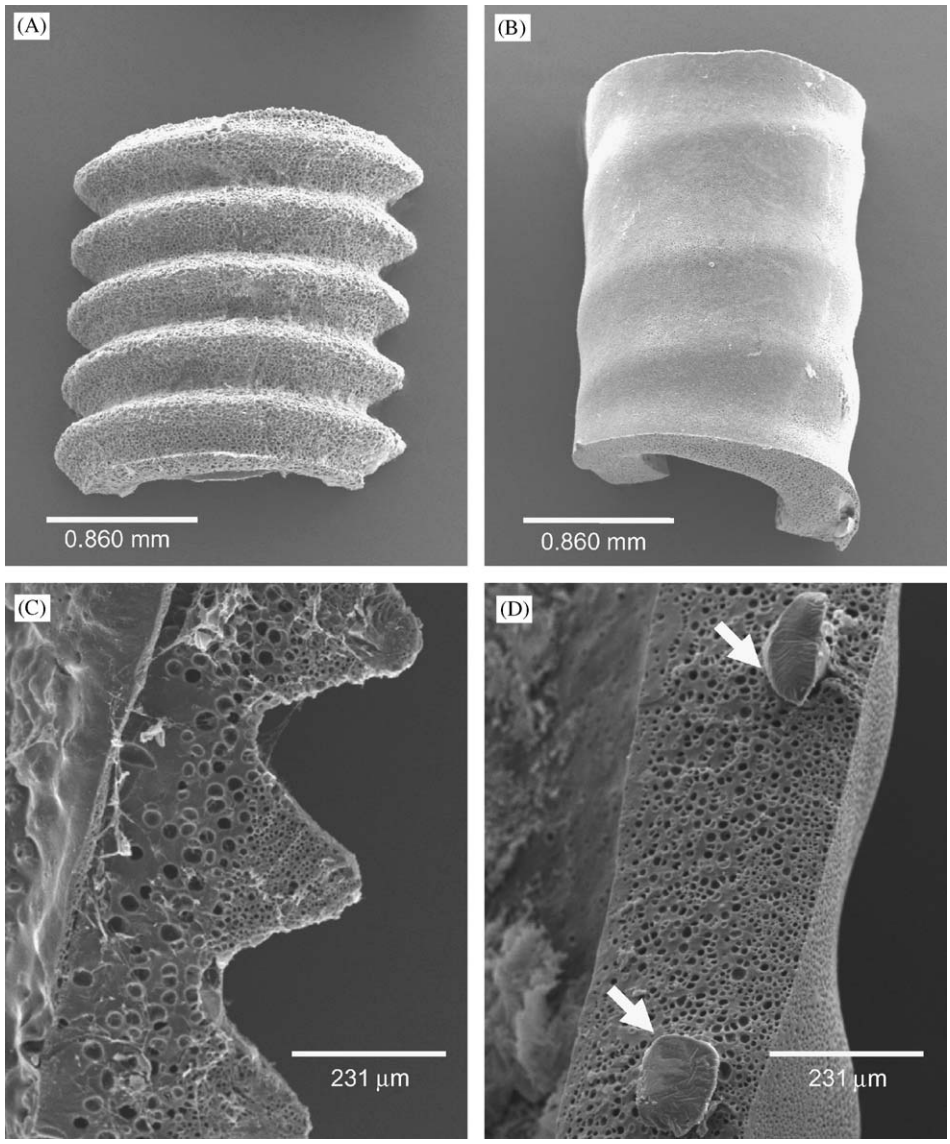

Fig. 1. Representative SEM micrographs of tubes synthesized by SpinFX® technology: (A) corrugated tube, (B) coil-reinforced tube, (C) 130x magnification of the corrugated tube wall, and (D) 130 × magnification of the coil-reinforced tube wall (arrow indicates coil).

including the autograft group; however, the autograft out-performed the tube groups at 8 weeks in terms of mean MAP velocity. As shown in Fig. 4, there was no statistically significant difference in the mean NAP velocity and the mean MAP velocity after 16 weeks in vivo between all groups studied, including the autograft, except the plain tube which demonstrated significantly poorer NAP velocity relative to both corrugated and coil-reinforced tubes. Interestingly, while the coil-reinforced tubes and autografts showed similar performance, the coil-reinforced tubes had a greater mean NAP velocity relative to autografts, yet the difference was not statistically significant.

Lateral gastrocmenius dry muscle mass also reflects functional nerve recovery because it is innervated by axons from the regenerated nerve cable and without this innervation, the muscle mass will decrease significantly [38]. As shown in Fig. 5, there was no statistical difference calculated for muscle mass among all groups studied at both 8 and 16 weeks, including the autograft group.

3.4. Histomorphometry

The overall tube geometry at explantation (i.e. patency, cf. Table 1), in vitro mechanical testing (Fig. 2) and the 16-week electrophysiological data (Fig. 4) together suggested that of the tube groups studied, the coil-reinforced tubes had superior performance to the other tube groups. It is for this reason that histomorphometry was done for this group only and compared to that for the autograft control at both 8 and 16 weeks

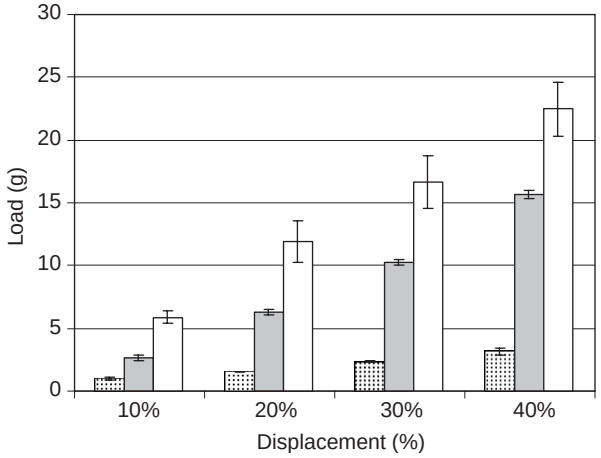

Fig. 2. Load vs. displacement graph reflects compressive strength the three tubes compared in vivo: plain tubes (▭) vs. corrugated (▬) vs. coil-reinforced tubes (▭). Each bar is significantly different from the other ($p<0.05$). ($n=3$, mean ± standard deviation).

Table 1
Tube patency was associated with the presence of a regenerating cable at 8- and 16-week explantation of grafts

Tube type	Time in vivo (n)[a]	Tube morphology			Regenerating cable
		Round	Oval	Collapsed	
Plain	8 wks (6)	4	2	0	4
	16 wks (6)	4	2	0	6
Corrugated	8 wks (6)	3	3	0	5
	16 wks (6)	4	0	2	6
Coiled	8 wks (6)	6	0	0	5
	16 wks (6)	6	0	0	6

[a] n is sample size.

(Figs. 6–10). As shown in Fig. 6, a thick regenerating cable (RC) filled the tube at 16 weeks and contained a diverse population of myelinated axons, where the myelin is easily observed as the black outline surrounding the axon (white core).

The regenerating cables in both 8- and 16-week coil-reinforced tubes were analysed and compared to those in autograft controls. As shown in Fig. 7 for the 8-week data, there was no statistically significant difference at either the mid-graft or distal nerve between the tube and autograft in terms of mean fibre diameter, mean fibre area, and total axon number per fascicle; however, in the coil-reinforced tubes, the G-ratio (i.e. axon diameter to fibre diameter) and the ratio of axon area to myelin area was greater in the mid-graft level for the tubes vs. the autografts.

As shown in Fig. 8 for the 16-week data, there was no statistically significant difference at either the mid-graft or distal nerve between the tube and autograft in terms of any of the parameters measured. This demonstrated equivalence in terms of regenerative performance of the coil-reinforced synthetic guidance channel and the autograft.

The distribution of fibre diameters within the distal nerve and the mid-section of the tube and autograft were compared at 8 and 16 weeks. As shown in Fig. 9, the majority of fibres had diameters ranging between 2.0 and 4.8 μm in both mid and distal segments of the nerve at 8 weeks for both autografts and coil-reinforced tubes. As shown in Fig. 10, the majority of fibres had diameters between 2.2 and 5.4 μm in both mid and distal segments of the nerve at 16 weeks for both autografts and coil-reinforced tubes. The overall fibre diameters were greater at 16 weeks relative to 8 weeks due to increased maturation of the nerve fibre.

4. Discussion

Corrugated and coil-reinforced tubes were synthesized in an attempt to overcome the limited patency previously observed with plain PHEMA-MMA tubes implanted as nerve guidance channels in the transected rat sciatic nerve [23]. The minimum mechanical properties required for tubes implanted in the sciatic nerve remain unknown as the compressive forces exerted on the tubes in vivo is uncertain. However, from the in vitro mechanical properties calculated in Fig. 2 and the fact that all coil-reinforced tubes remained patent at 16 weeks whereas some corrugated tubes collapsed at 16 weeks, one may speculate that the minimum mechanical properties required for patency in the peripheral nerve graft falls somewhere between those of corrugated and coil-reinforced tubes. While both corrugated and coil-reinforced tubes had greater compressive strength (Fig. 2) than the plain tubes, only the coil-reinforced tubes demonstrated consistently better patency (Table 1), which in turn affected the regenerating cable.

The idea of enhancing compressive strength with corrugation or coils has been studied in some biomedical [26–29] and numerous industrial applications [30–32]; however, coiled tubes have not been studied as nerve guidance channels. Other ways to increase the mechanical strength of the tube is to increase MMA content or increase the wall thickness. However, there are practical limitations in terms of monomer and MMA concentrations in terms of solubility. Moreover, merely "hardening" the material will decrease tube flexibility which may cause tissue necrosis due to a mismatch in tissue and implant mechanical properties. Using the corrugated or coil-reinforced design allows the tube to have greater mechanical strength while preserving the inherent modulus of the material that is similar to the soft tissue in which the tubes are implanted.

The permeability of the nerve guidance channel is known to impact regeneration within where non-permeable tubes, such as silicones, show poorer regeneration

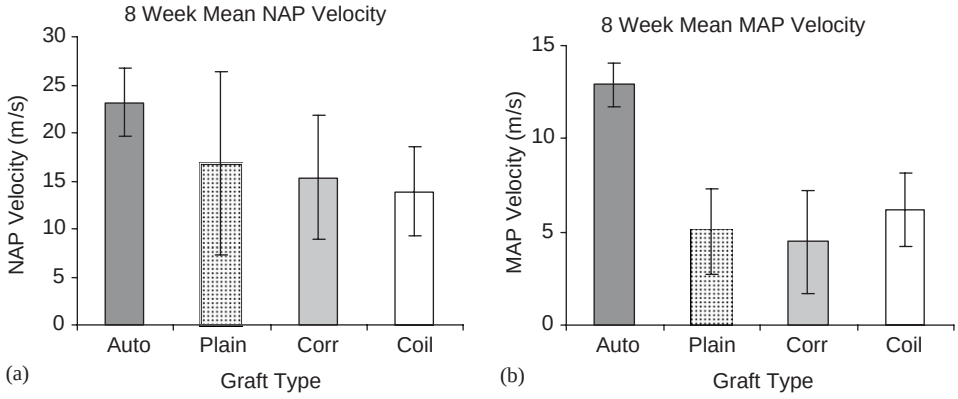

Fig. 3. Summary of electrophysiology data at 8 weeks. (a) mean nerve action potential (NAP) velocity (±standard deviation) and (b) mean muscle action potential (MAP) velocity (±standard deviation).

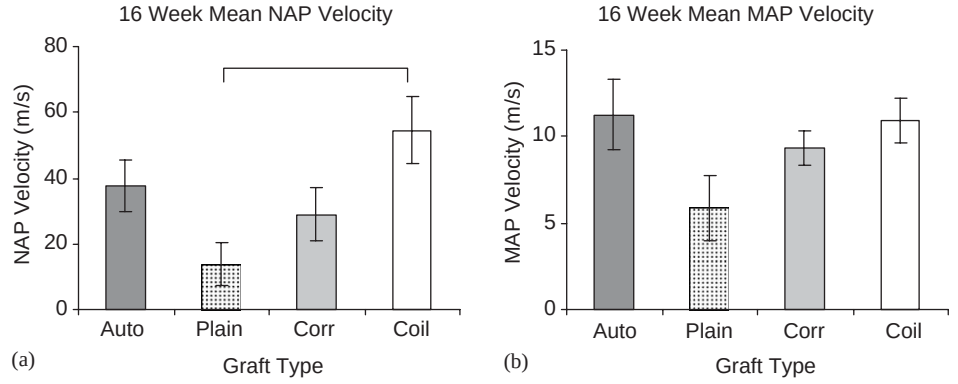

Fig. 4. Summary of electrophysiology data at 16 weeks. (a) mean nerve action potential (NAP) velocity and (b) mean muscle action potential (MAP) velocity (± standard deviation), Brackets above bars indicate the statistically significant difference between connected groups ($p<0.05$).

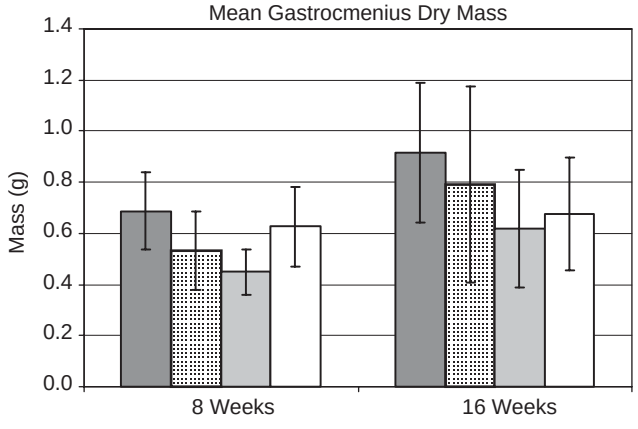

Fig. 5. Mean lateral gastrocmenius muscle dry mass after (a) 8 weeks and (b) 16 weeks of autograft (■), plain tube (□), corrugated tube (▭) and coil-reinforced tube (▭) implantation (± standard deviation).

than porous guidance channels such as collagen [39–41]. Permeability is important because as the axons regenerate through the tubes, the metabolic activities of the cells necessitate the exchange and transport of nutrients and wastes between inside and outside of the tube. In these studies, all tubes were synthesized with the same formulation and it was only the design that was changed. Since permeability across the membrane is impacted by wall morphology and thickness, which are influenced by formulation chemistry, it is reasonable to assume that permeability across all three tubular constructs—plain, corrugated and coil-reinforced—were similar. Based on previous published data [25], we anticipate that the PHEMA-MMA tubes described herein have similar diffusion coefficients to those tubes previously studied, where diffusion coefficient of, for example, 10 kDa dextran was $0.531 \pm 0.103 \times 10^{-8}\,cm^2\,s^{-1}$. We anticipate that the diffusion coefficient of FGF-1 will be lower than that of 10 kDa dextran and thus retained longer in the tubes while small wastes and nutrients are readily exchanged.

In some of the previous 16-week tubes where some collapse was observed, we did not know whether the lack of a regenerating cable within the tubes was due to collapse or whether tube collapse was a consequence of

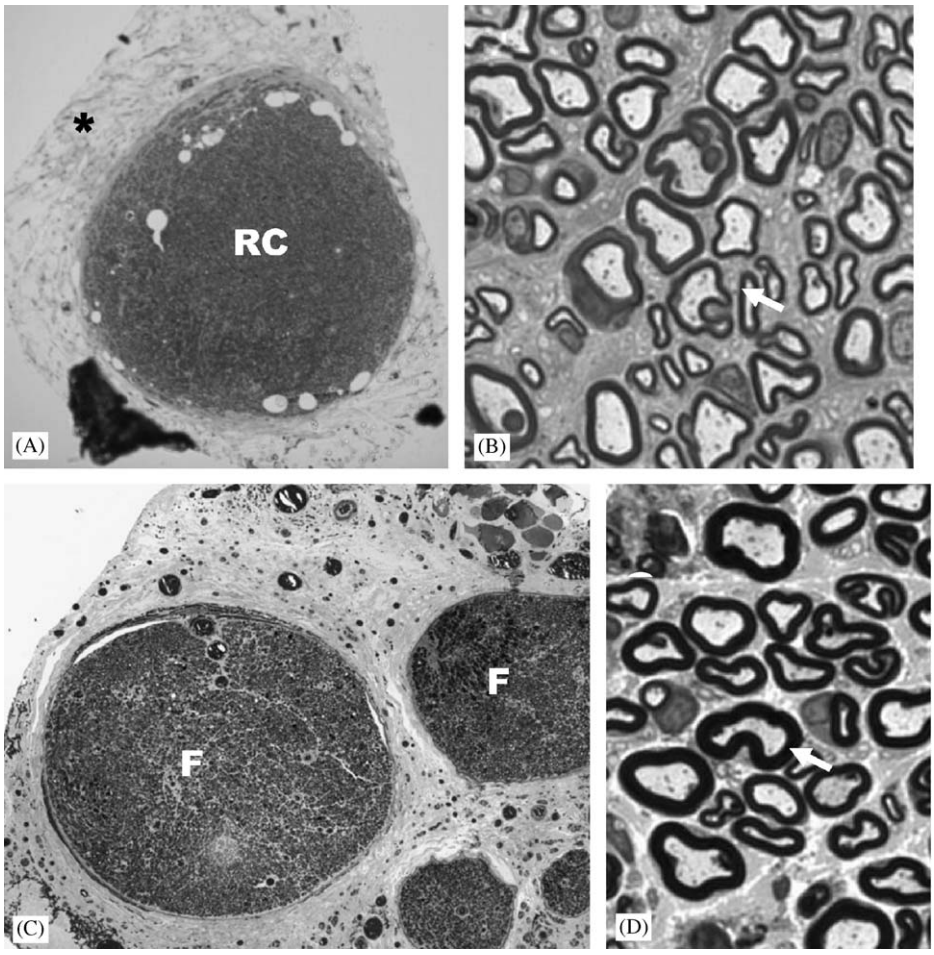

Fig. 6. Cross section of the mid section of grafts at 16 weeks: (A) 40 × magnification of the regenerating cable (RC) with in the tube, (B) 100 × magnification of the regenerating cable, (C) 40 × magnification of the autograft and (D) 100 × magnification of the autograft section. ''*'' indicates the tube wall. Arrow indicates myelinated axon. F is the fascicle of the autograft.

the lack of a regenerating cable [17]. We hypothesized that better mechanical integrity would improve overall patency of the tubes for long-term regeneration studies, as was indeed demonstrated.

To gain greater insight into the correlation of tube patency and the presence of a regenerating cable, we noted that a regenerating cable was present in all tubes after 16 weeks, irrespective of collapse, but not after 8 weeks, where there was some correlation between the presence of a regenerating cable and patency. It is important to realize that not all regenerating cables are the same. Indeed, some regenerating cables had a higher density of axons than others, and some cables were smaller than others. We therefore relied on quantitative functional outcome measures (electrophysiology, reinnervated muscle mass and histomorphometry) to gain greater insight into the differences observed between the tube groups studied [37].

Nerve regeneration through a tube is divided into five stages [42,43]: (1) within the first day, the inner lumen of the tube is filled with fluid containing neurotrophic factors; (2) then, between days 2 and 6, an acellular fibrin matrix forms to bridge the distal and proximal stumps; (3) this is followed between days 7 and 14 with Schwann cells and endothelial cells that infiltrate the tube lumen from both proximal and distal stumps: (4) then, between 15 and 21 days, axons begin to grow from the proximal stump, increase in size and become myelinated; (5) lastly, after 21 days (depending on gap and tube length), regenerating axons from the proximal stump enter the distal stump.

Electrophysiological activity at 8 weeks indicates the presence of some population of axons in the regenerating cable for all the tube groups (cf. Fig. 4). This implies that tubes were open for at least 3 weeks to support axonal regeneration, and that the collapsing that was observed in a subset of tubes occurred between 3 and 8 weeks, after the regenerating cable had already formed. The electrophysiological data at 16 weeks correlates directly with the ''round'' tube geometry and the presence of a regenerating cable, but does not correlate with the collapsed tube, as was observed for two of the

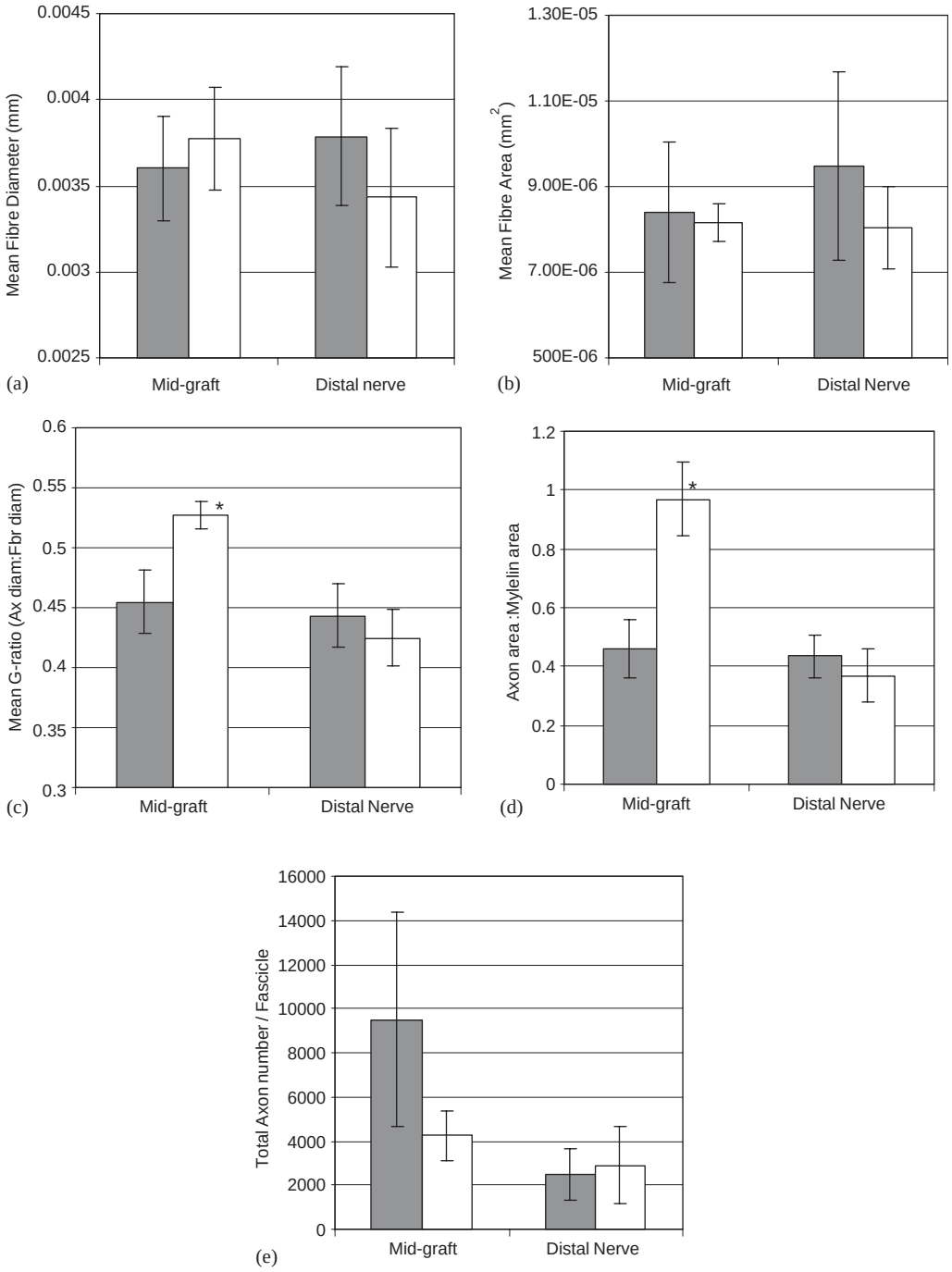

Fig. 7. Summary of 8-week histomorphometry data for autograft (▬) and coil-reinforced tube (▭) groups; (a) mean fibre diameter, (b) mean fibre area, (c) mean G-ratio, (d) Axon area:myelin area, (e) total axon number per area of fascicle (± standard deviation). "*" indicates the statistically significant difference between the group.

corrugated tubes. While the mean NAP velocity was lower for the corrugated tube than the coil-reinforced tube, the plain tubes showed the poorest results and were statistically different. For mean MAP velocity, no differences existed in corrugated and coil-reinforced tubes yet plain tubes performed statistically worse. Unfortunately, weighing the lateral gastrocmenius muscle did not show any differences between the repair groups and this may reflect surgical errors in dissecting out the tissue or weighing the "blotted" dry samples, as large standard deviations are reported.

Histomorphometry helped to complete the picture of regeneration thorough synthetic nerve guidance channels relative to autografts. The regenerating cable was filled with myelinated axons (cf. Fig. 6) and between 8 and 16 weeks, fibres within the coil-reinforced tubes

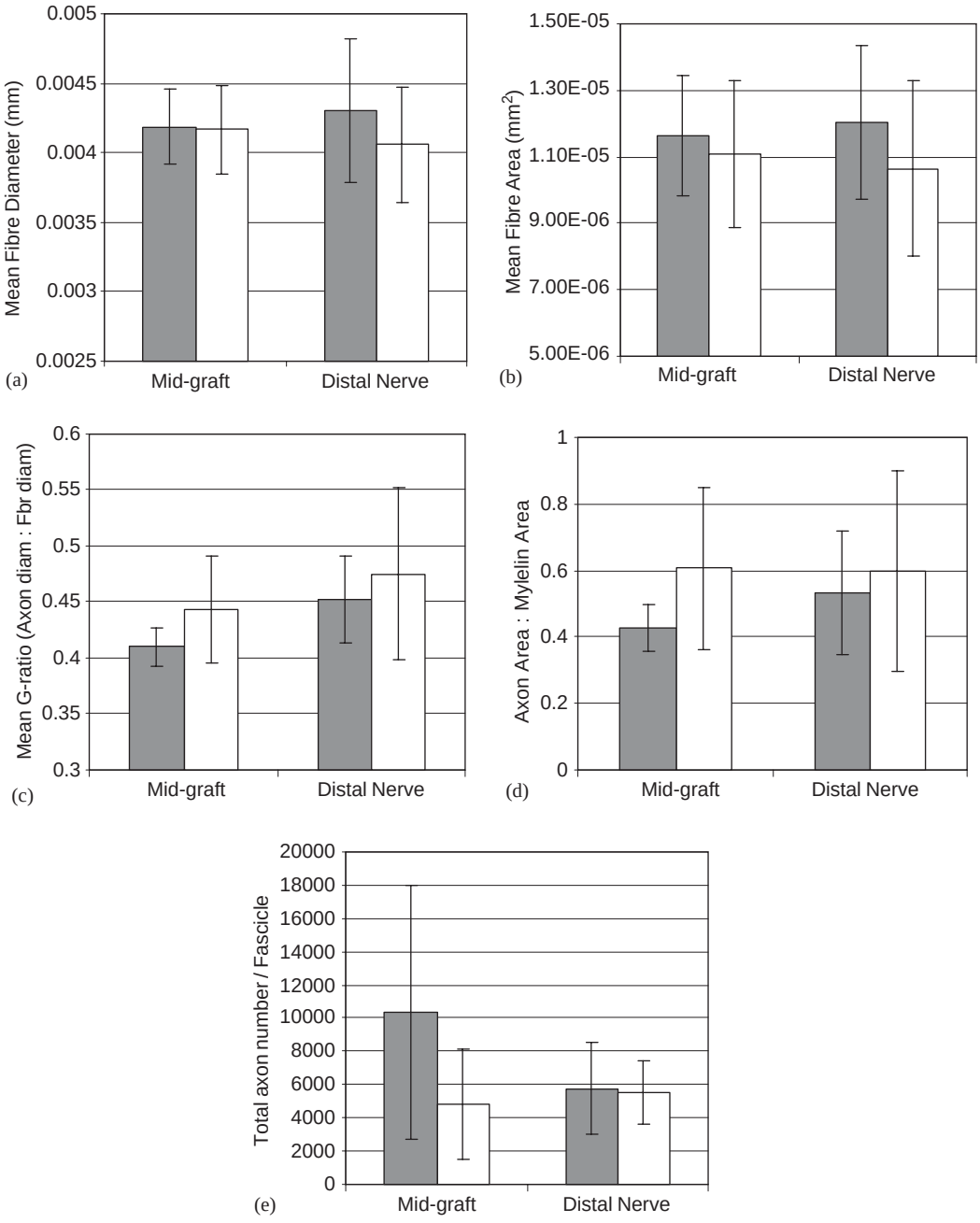

Fig. 8. Summary of 16-week histomorphometry data for autograft (▬) and coil tube (⌐) groups; (a) mean fibre diameter, (b) mean fibre area, (c) mean G-ratio, (d) axon area:myelin area, (e) total axon number per area of fascicle (±standard deviation).

(and autografts) continued to mature. As indicated in the fibre diameter histogram (Figs. 9b and 10b), there was a larger population of fibres above 5.00 μm in diameter after 16 weeks. It is generally understood that the larger diameter axon demonstrates faster nerve conduction. The comparison of histomorphometry data showed that most of the parameters were not statistically different from each other in both 8 and 16 weeks, except for G-ratio and ratio of axon area to myelin area (Fig. 7), where the coil-reinforced synthetic tube group out-performed the autograft in the mid-graft level and approached normal G-ratio values of 0.50 and 0.55 at 8 weeks [44,45]. At 16 weeks, the mean G-ratio was lower than normal in both autograft and coil-reinforced tube groups. The G-ratio of healthy nerves was reported between 0.6 and 0.7 in rat tibial and sciatic nerves and monkey median nerves [22,46–49]. G-ratio represents the relationship of axon and myelin, which impacts on conduction velocity of the nerve, and the fibres with the optimum velocity have G-ratios between 0.6 and 0.7 [48].

The conduction velocity of the healthy peripheral nerve varies with the types of nerves. The fastest

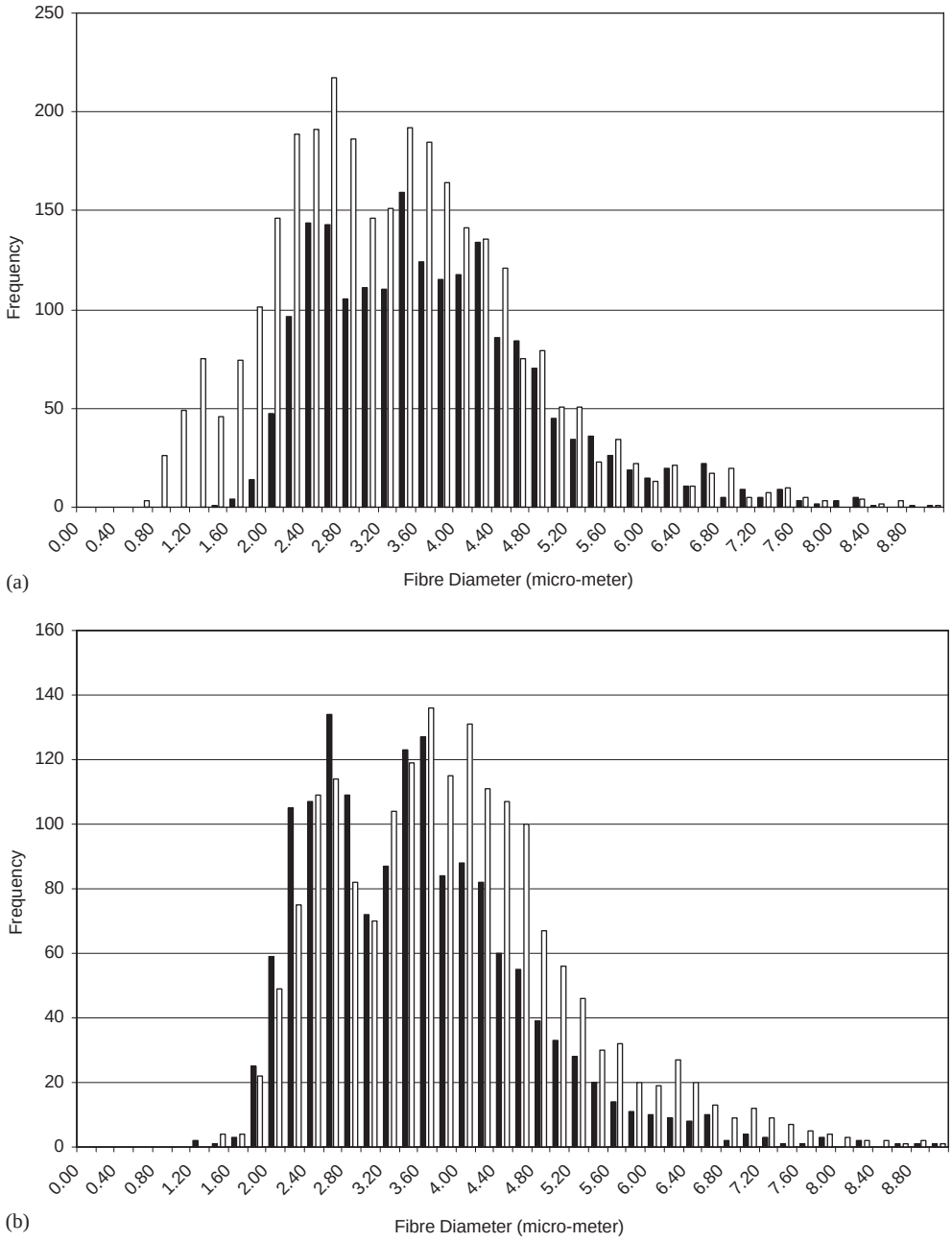

Fig. 9. Total fibre diameter distribution within regenerating cables at 8 weeks ($n = 6$): (a) fibre diameter distribution from autograft; mid section of the graft (▭) and distal nerve (■), and (b) fibre diameter distribution from coil; mid section of the graft (▭) and distal nerve (■).

conducting nerves are type Ia, Ib and α, which are sensory fibres from muscles, tendon organs and skeletomotor nerves, respectively, where conduction velocity is between 50 and 110 m/s [50]. The fibre diameters of these nerves range between 9 and 20 μm. The next fastest conducting nerves are type II and β, which are skeletomotor and fusimotor nerves, and show characteristic conduction velocities between 20 and 85 m/s with fibre diameters between 5 and 15 μm [50]. Our study showed an average NAP velocity of 54 ± 10.1 m/s of the coil-reinforced group at 16 weeks, which is within the range of healthy nerves. Another study showed that the conduction velocity of healthy rat sciatic nerve was 54.0 ± 0.7 m/s, which is comparable to our results [51].

Although a sub-population of fibre diameters fell between 5.4 and 9.0 μm, the majority of the population was between 2.0 and 4.8 μm in the present study. The fibre diameter of the normal healthy fibre is reported to be 7.25 ± 0.39 μm in rat sciatic nerve and 7.81 ± 0.60 μm in monkey median nerve [22,52]. However, the reduction of the fibre diameter and increase in number of fibres are expected in regenerating sciatic nerves, as the fibre

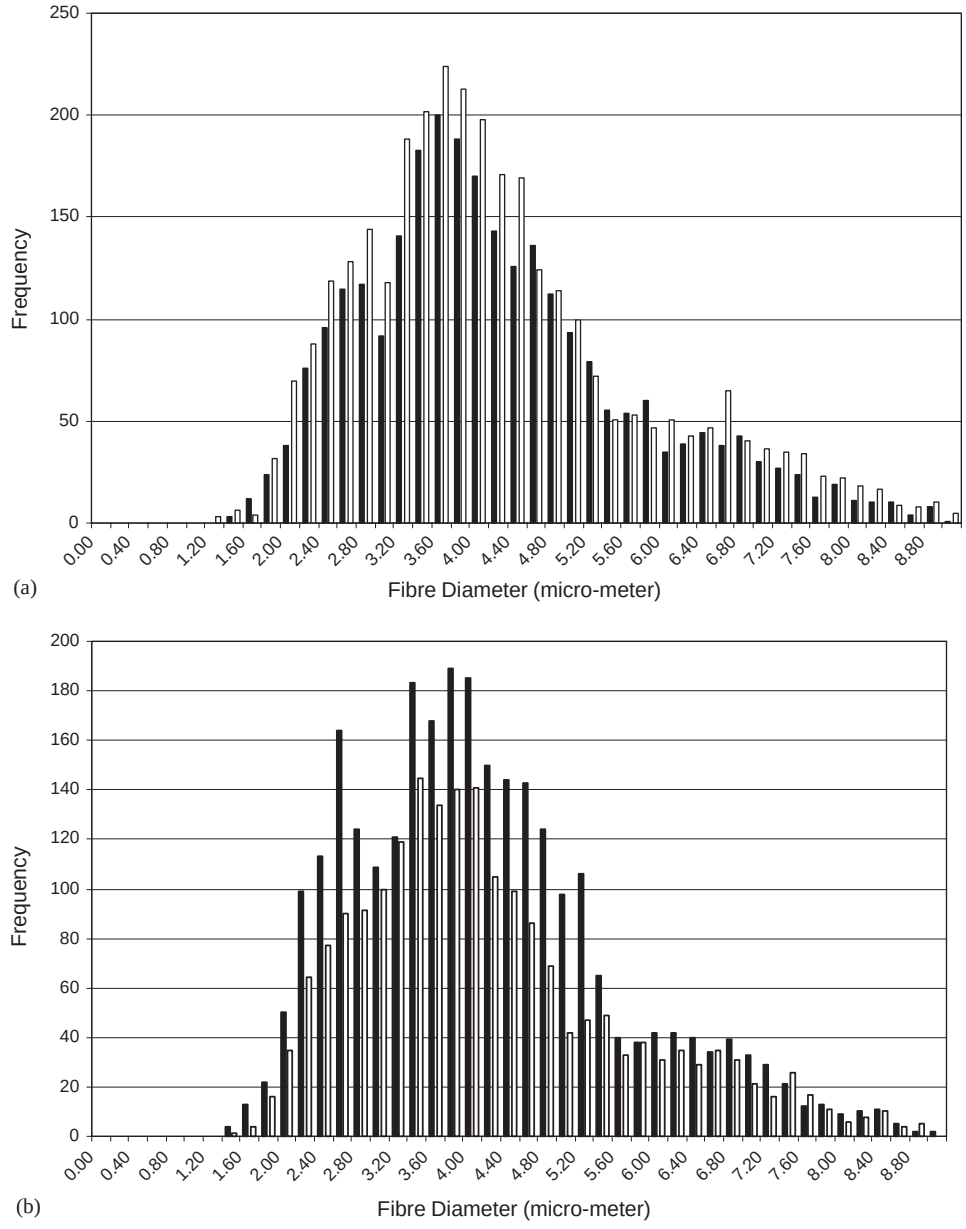

Fig. 10. Total fibre diameter distribution within regenerating cables at 16 weeks ($n = 6$): (a) fibre diameter distribution from autograft; mid section of the graft (⊓) and distal nerve (■), (b) fibre diameter distribution from coil; mid section of the graft (⊓) and distal nerve (■).

branches out during regeneration [52]. In fact, in a variety of entubulation strategies, where the tubes were synthesized from silicone, collagen, poly(L-lactide-*co*-ε-caprolactone) and Goretex (with or without added neurotrophic factors), regenerated axon diameters were no greater than 5 μm, while the control uninjured healthy axons had diameters greater than 7 μm [53–55].

5. Conclusions

The coil-reinforced PHEMA-MMA nerve guidance channels demonstrated equivalence to nerve autografts (the current "gold" standard) in a 10 mm rat transected peripheral nerve injury model, as assessed by several validated outcome measures of nerve regeneration. The coil-reinforced composite tubes provide a new design strategy to create tubes with mechanical integrity from low modulus materials, such as hydrogels, that match the modulus of soft tissues. These strategies could be applied to other device designs and indicate that nerve autografts can be replaced with synthetic alternatives. While there is significant precedence for the use of non-degradable polymers in both peripheral nerve and spinal cord repair strategies, as is described here for PHEMA-MMA nerve guidance channels, there is a general desire

to use degradable tubes, thereby obviating the need for a second surgery to remove the nerve guidance channel after regeneration is complete. In ongoing studies we are investigating the use of degradable polymeric tubes in both spinal cord and peripheral nerve repair strategies.

Acknowledgements

We thank matREGEN Corp and the Advanced Regenerative Tissue Engineering Centre, an Ontario Research and Development Challenge Fund-sponsored center for funding. We are grateful to Qing Gui Xu (RM & MSS, CIHR MOP-53221) for performing the surgeries and helpful discussions. We thank Maria Jimenez-Hamann for helping to prepare the collagen solution that filled the tubes and William Chung for preparing the coil-reinforced tubes.

References

[1] Silver J, Miller JH. Regeneration beyond the glial scar. Nat Rev Neurosci 2004;5:146–56.
[2] Tsai E, Dalton PD, Shoichet MS, Tator CH. Synthetic hydrogel guidance channels facilitate regeneration of adult rat brainstem motor axons after complete spinal cord transection. J Neurotrauma 2004;21:789–804.
[3] Guest JD, Rao A, Olson L, Bunge MB, Bunge RP. The ability of human Schwann cell grafts to promote regeneration in the transected nude rat spinal cord. Exp Neurol 1997;148:502–22.
[4] Xu XM, Guenard V, Kleitman N, Bunge MB. Axonal regeneration into schwann cell-seeded guidance channels grafted into transected adult-rat spinal-cord. J Comp Neurol 1995;351:145–60.
[5] Bunge MB. Transplantation of purified populations of schwann-cells into lesioned adult-rat spinal cord. J Neurol 1994;242:S36–9.
[6] Patist CM, Mulder MB, Gautier SE, Maquet V, Jerome R, Oudega M. Freeze-dried poly(D,L-lactic acid) macroporous guidance scaffolds impregnated with brain-derived neurotrophic factor in the transected adult rat thoracic spinal cord. Biomaterials 2004;25:1569–82.
[7] Waller A. Experiments on the section of the glossopharyngeal and hypoglossal nerves of the frog, and observations of the alterations produced thereby in the structure of their primitive fibres. Philos Trans Roy Soc (Lond) 1850;140:423–9.
[8] Morris JH. An electron microscope study of degeneration and regeneration in mammalian peripheral nerves. University of Oxford Thesis/Dissertation 1971.p.I–173.
[9] Morris JH, Hudson AR, Weddell G. A study of degeneration and regeneration in the divided rat sciatic nerve based on electron microscopy. III. Changes in the axons of the proximal stump. Z Zellforsch Mikrosk Anat 1972;124:131–64.
[10] Bratton BR, Kline DG, Coleman W, Hudson AR. Experimental interfascicular nerve grafting. J Neurosurg 1979;51:323–32.
[11] Hudson AR, Hunter DA, Kline DG, Bratton BR. Histological studies of experimental interfascicular graft repairs. J. Neurosurg 1979;51:333–40.
[12] Wong AYC, Scott JJA. Functional recovery following direct or graft repair of nerve gaps in the rat. Exp Neurol 1991;114:364–6.
[13] Ortiguela ME, Wood MB, Cahill DR. Anatomy of the sural nerve complex. J Hand Surg 1987;12A:1119–23.
[14] Mackinnon SE, Hudson AR. Clinical application of peripheral nerve transplantation. Plast Reconstr Surg 1992;90:695–9.
[15] Mackinnon SE, Dellon AL. Surgery of the peripheral nerve. New York: Thieme Medical Publishers; 1988.
[16] Millesi H. Reappraisal of nerve repair. Surg Clin North Am 1981;61:321–40.
[17] Belkas JS, Munro CA, Shoichet MS, Johnston M, Midha R. Long-term in vivo biomechanical properties and biocompatibility of poly(2-hydroxyethylmethacrylate-*co*-methyl methacrylate) nerve conduits. Biomaterials 2005;26:1741–9.
[18] Meek MF, van der Werff JFA, Klok F, Robinson PH, Nicolai JPA, Gramsbergen A. Functional nerve recovery after bridging a 15 mm gap in rat sciatic nerve with a biodegradable nerve guide. Scand J Plast Reconstr Surg Hand Surg 2003;37:258–65.
[19] Varejao ASP, Cabrita AM, Geuna S, Patricio JA, Azevedo HR, Ferreira AJ, et al. Functional assessment of sciatic nerve recovery: biodegradable poly (DLLA-e-CL) nerve guide filled with fresh skeletal muscle. Microsurgery 2003;23:346–53.
[20] Li ST, Archibald SJ, Krarup C, Madison RD. Peripheral nerve repair with collagen conduits. Clin Mater 1992;9:195–200.
[21] Archibald SJ, Krarup C, Shefner J, Li ST, Madison RD. A collagen-based nerve guide conduit for peripheral nerve repair: an electrophysiological study of nerve regeneration in rodents and nonhuman primates. J Comp Neurol 1991;306:685–96.
[22] Archibald SJ, Krarup C, Shefner J, Li ST, Madison RD. Monkey median nerve repaired by nerve graft or collagen nerve guide tube. J Neurosci 1995;15:4109–23.
[23] Belkas JS, Munro CA, Shoichet MS, Midha R. Peripheral nerve regeneration through a synthetic hydrogel nerve tube. Restorative Neurol Neurosci 2005;23:19–29.
[24] Dalton PD, Shoichet MS. Creating porous tubes by centrifugal forces for soft tissue application. Biomaterials 2001;22:2661–9.
[25] Luo Y, Dalton PD, Shoichet MS. Investigating the properties of novel poly(2-hydroxyethyl methacrylate-*co*-methyl methacrylate) hydrogel hollow fiber membranes. Chem Mater 2001;13:4087–93.
[26] Caro C, Jeremy J, Watkins N, Bulbulia R, Angelini G, Smith F, et al. The geometry of unstented and stented pig common carotid artery bypass grafts. Biorheology 2002;39:507–12.
[27] Bunc G, Kovacic S, Strnad S. Evaluation of functional response of cerebral arteries by a new morphometric technique. Auton Neurosci 2001;93:41–7.
[28] Cole MW, Crespi VH, Stan G, Ebner C, Hartman JM, Moroni S, et al. Condensation of helium in nanotube bundles. Phys Rev Lett 2000;84:3883–6.
[29] Sheet steel: carbon, high strength low alloy, alloy, uncoated, metallic coated, coil coated, coils, cut lengths, corrugate products. Iron and Steel Society, 1999.
[30] Abdel-Sayed G. Soil–steel bridges: design and construction. New york; 1993.
[31] Selves NW. Profiled sheet roofing and cladding: a guide to good practice. E & FN Spon; 1999.
[32] Seckel BR. Enhancement of peripheral nerve regeneration. Muscle & Nerve 1990;13:785–800.
[33] Midha R, Munro CA, Dalton PD, Tator CH, Shoichet MS. Growth factor enhancement of peripheral nerve regeneration through a novel synthetic hydrogel tube. J Neurosurg 2003;99:555–65.
[34] Midha R, Evans PJ, Mackinnon SE, Best TJ, Hare GMT, Hunter DA, et al. Comparison of regeneration across nerve allografts with temporary or continuous Cyclosporin A immunosupression. J Neurosurg 1993;78:90–100.
[35] Midha R, Munro CA, Dalton PD, Tator CH, Shoichet MS. Peripheral nerve regeneration through a novel synthetic hydrogel nerve tube is enchanced by growth factors. J Neurosurg 2003;99:555–65.
[36] Evans PJ, Mackinnon SE, Midha R, Wade JA, Hunter DA, Nakao Y, et al. Regeneration across cold preserved peripheral nerve allografts. Microsurgery 1999;19:115–27.

[37] Munro CA, Szalai JP, Mackinnon SE, Midha R. Lack of association between outcome measures of nerve regeneration. Muscle Nerve 1998;21:1095–7.
[38] Hoenger A, Doerhoefer M, Woehlke G, Tittmann P, Gross H, Song YH, et al. Surface topography of microtubule walls decorated with monomeric and dimeric kinesin constructs. Biol Chem 2000;381:1001–11.
[39] Widmer MS, Gupta PK, Lu LC, Meszlenyi RK, Evans GRD, Brandt K, et al. Biomaterials 1998;19:1945–55.
[40] Evans GRD, Brandt K, Widmer MS, Lu L, Meszlenyi RK, Gupta PK, et al. Biomaterials 1999;20:1109–15.
[41] Rutkowski GE, Heath CA. Development of a bioartificial nerve graft. II. Nerve regeneration in vitro. Biotechnol Progr 2002;18: 373–9.
[42] Heath CA, Rutkowski GE. The development of bioartificial nerve grafts for peripheral-nerve regeneration. Trends Biotechnol 1998;16:163–8.
[43] Donaldson HH, Hoke GW. On the areas of the axis cylinder and medullary sheath as seen in cross sections of the spinal nerves of vertebrates. J Comp Neurol Psychol 1905;15:1–16.
[44] Greenman MJ. Studies on the regeneration of the peroneal nerve of the albino rat: number and sectional areas of fibres: area relation of axis to sheath. J Comp Neurol 1913;23:479–513.
[45] Fraher JP, O'Leary D, Moran MA, Cole M, King RHM, Thomas PK. Relative growth and maturation of axon size and myelin thickness in the tibial nerve of the rat. Acta Neuropathol 1990;79:364–74.
[46] Fansa H, Schneider W, Wolf G, Keilhoff G. Influence of insulin-like growth factor-I (IGF-I) on nerve autografts and tissue-engineered nerve grafts. Muscle Nerve 2002;26:87–93.
[47] Ahmed Z, Brown RA, Ljungberg C, Wiberg M, Terenghi G. Nerve growth factor enhances peripheral nerve regeneration in non-human primates. Scand J Plast Reconstr Hand Surg 1999;33:393–401.
[48] Ansselin AD, Fink T, Davey DF. An alternative to nerve grafts in peripheral nerve repair: nerve guides seeded with adult Schwann cells. Acta Chururgica Austriaca 1998;30:19–24.
[49] Landon DN. The Peripheal Nerve. New York: Wiley; 1976. p. 2–4.
[50] van Meeteren NLU, Brakkee JH, Hamers FPT, Helders PJM, Gispen WH. Exercise training improves functional recovery and motor nerve conduction velocity after sciatic nerve crush lesion in the rat. Arch Phys Med Rehabil 1997;78:70–7.
[51] Vleggeert-Lankam- CLAM, van den Berg RJ, Feirabend HKP, Lakke EAJF, Malessy MJA, Thomeer RTWM. Electrophysiology and morphometery of the Aa- and Ab-fibre populations in the normal and regenerating rat sciatic nerve. Exp Neurol 2004;187:337–49.
[52] Xu X, Yee WC, Hwang PY, Yu H, Wan AC, Gao S, et al. Peripheral nerve regeneration with sustained release of poly(phosphoester) microencapsulated nerve growth factor within nerve guide conduits. Biomaterials 2003;24:2405–12.
[53] Dowsing BJ, Hayes A, Bennett TM, Morrison WA, Messina A. Effects of LIF dose and laminin plus fibronectin on axotomized sciatic nerves. Muscle Nerve 2000;23:1356–64.
[54] Chamberlain LJ, Yannas IV, Hsu HP, Strichartz GR, Spector M. Near-terminus axonal structure and function following rat sciatic nerve regeneration through a collagen-GAG matrix in a ten-millimeter gap. J Neurosci Res 2000;60:666–77.
[55] Matsumoto K, Ohnishi K, Kiyotani T, Sekine T, Ueda H, Nakamura T, et al. Peripheral nerve regeneration across an 80-mm gap bridged by a polyglycolic acid (PGA)-collagen tube filled with laminin-coated collagen fibers: a histological and electrophysiological evaluation of regenerated nerves. Brain Res 2000;868:315–28.